LSSC: Lensing Super Sample Covariance

Akira Tokiwa,[1,2,3]★ Adrian Bayer,[1] Masahiro Takada[1,2,3] Jia Liu[1,3]
[1]Kavli Institute for the Physics and Mathematics of the Universe (WPI), 5-1-5 Kashiwanoha, Kashiwa-shi, Chiba, 277-8583, Japan
[2]Department of Physics, The University of Tokyo, 7-3-1 Hongo, Bunkyo-ku, Tokyo 113-0033 Japan
[3]Center for Data-Driven Discovery, Kavli IPMU (WPI), UTIAS, The University of Tokyo, Kashiwa, Chiba 277-8583, Japan

Accepted XXX. Received YYY; in original form ZZZ

ABSTRACT

we study the effect of super sample covariance (SSC) on the weak lensing statistics. We use a set of N-body simulations to quantify the SSC effect on the convergence power spectrum, peak counts, minimum counts, and the scattering transform. We find that the SSC effect is negligible for the convergence power spectrum and higher order statistics. We discuss the implication of our results for the future weak lensing surveys such as Euclid and Rubin Observatory Legacy Survey of Space and Time (LSST).

Key words: keyword1 – keyword2 – keyword3

1 INTRODUCTION

2 METHODS

2.1 Covariance

almost copy from the paper of Bayer et al. (2023)

The covariance matrix between an observable O_α and another observable O_β is given by

$$C_{\alpha\beta} = (\langle O_\alpha - \langle O_\alpha \rangle \rangle) \left(\left\langle O_\beta - \left\langle O_\beta \right\rangle \right\rangle\right) \quad (1)$$

$\langle\rangle$ denotes the mean over the realizations. $C_{\alpha\beta}$ can be estimated by using an ensemble of simulations of different realizations of the initial conditions.

We quantify the SSC effect by comparing the following two sets of simulations:

- lightcone of sub-boxes that extract from a much larger simulation box, captures super-sample mode $\theta > \theta_{max}$.
- lightcone of small-boxes that consists of tiled small boxes, independently simulated with periodic boundary conditions and only have mode $\theta \leq \theta_{max}$.

Because the Super sample modes are only present in the former and not in the latter, the SSC is given by

$$C_{SSC} = C_{sub} - C_{small} \quad (2)$$

where C_{sub} is the covariance computed using sub-boxes and C_{small} is that using small boxes.

2.2 Ray Traced Weak Lensing Map

almost copy from the paper of Osato et al. (2021)

To build a light cone, we stacked the snapshots along the line-of-sight in an interval of $500 Mpc/h$, which is the size of the small boxes. The comoving distance is from $z = 0$ to $z \sim 1.65$. We summarize the light cone configuration in table 1. Here, the redshift is simply computed by using the comoving distance of the snapshot center with `Python` package `astropy`. The opening angle of the light cone is 5×5 deg^2.

Table 1. Summary of the light cone. Columns (1) snapshot number; (2) comoving distance and (3)redshift at the snap shot center.

# Snapshot	$\chi[Mpc/h]$	z
1	250	0.057
2	750	0.177
3	1250	0.305
4	1750	0.443
5	2250	0.593
6	2750	0.759
7	3250	0.942
8	3750	1.148
9	4250	1.382
10	4750	1.649

To model the propagation of light rays, we employ a multiple lens plane approximation, where the smooth matter distribution is approximated as discrete density planes of thickness $\Delta\chi$. Light rays originating from the observer at z = 0 are deflected only at the planes and travel in straight lines between the planes. At the angular position β^k at the k-th plane, the deflection angle α is the gradient of the 2D lensing potential ψ.

$$\alpha^k(\beta^k) = \nabla_{\beta^k} \psi^k(\beta^k) \quad (3)$$

The lensing potential can be computed from the Poisson equation:

$$\nabla^2_{\beta^k} \psi^k(\beta^k) = 2\sigma^k(\beta^k), \quad (4)$$

where the dimensionless surface density σ^k is the projected matter distribution of the k-th lens plane:

$$\sigma^k(\beta^k) = \frac{3H_0^2\Omega_m}{2c^2} \frac{\chi^k}{a^k} \int_{\chi^k+\Delta\chi/2}^{\chi^k-\Delta\chi/2} \delta(\beta^k, \chi)\, d\chi, \quad (5)$$

★ E-mail: akira.tokiwa@ipmu.jp

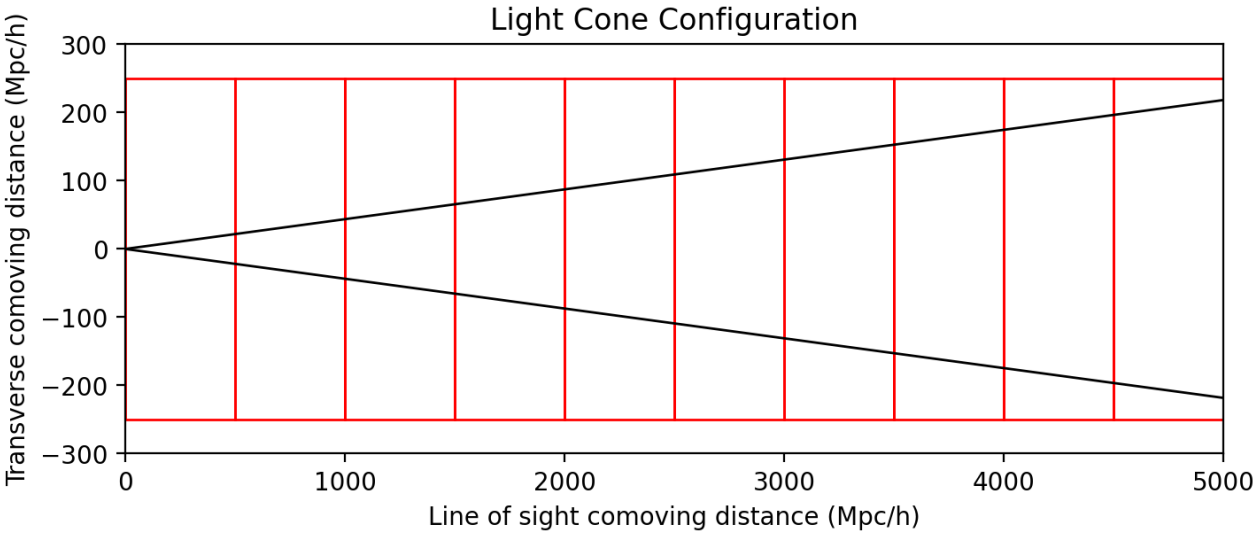

Figure 1. The construction of the light cone. Each red box corresponds to one snapshot. The black lines correspond to the opening angle of 5 deg.

where c is the speed of light, a is the scale factor, and $\delta = (\rho - \bar{\rho})/\bar{\rho}$ is the three-dimensional matter overdensity. The lensed position β^k is the sum of previous deflection angles:

$$\boldsymbol{\beta}^k(\boldsymbol{\theta}) = \boldsymbol{\theta} - \sum_{i=1}^{k-1} \frac{\chi^k - \chi^i}{\chi^k} \boldsymbol{\alpha}^i \left(\boldsymbol{\beta}^i\right), (k = 2, 3, \ldots) \tag{6}$$

where we impose $\boldsymbol{\beta}^0 = \boldsymbol{\beta}^1 = \boldsymbol{\theta}$. By differentiating $\boldsymbol{\beta}^k$ with respect to $\boldsymbol{\theta}$, we obtain the Jacobian matrix $\mathcal{A}$:

$$\mathcal{A}(\boldsymbol{\theta}, \chi) \equiv \frac{\partial \boldsymbol{\beta}}{\partial \boldsymbol{\theta}}(\boldsymbol{\theta}, \chi) = \begin{pmatrix} 1 - \kappa - \gamma_1 & -\gamma_2 + \omega \\ -\gamma_2 - \omega & 1 - \kappa + \gamma_1 \end{pmatrix} \tag{7}$$

where κ is the convergence, γ_1 and γ_2 are the two components of the shear, and ω is the rotation.

We apply a fast Fourier transform (FFT) to equation (2) to obtain the derivatives of the lensing potential ψ with respect to the angular position β^k. We evaluate the deflection and the Jacobian matrix at the angular position β^k and generate κ, γ_1, γ_2, and ω maps at the k-th lens plane. Note that k-th lens plane contains the matter distribution from the range $\left(\chi^k - \Delta\chi/2, \chi^k + \Delta\chi/2\right)$. but observables are defined at χ^k. Thus, the k-th source plane is placed at $\chi^k + \Delta\chi/2$.

3 STATISTICS

- Convergence Power Spectrum:
- PDF
- Peak
- minimum
- scattering transform
- Mass function

3.1 Convergence Power Spectrum

almost copy from the paper of Shirasaki et al. (2015)

Under flat sky approximation, the Fourier transform of the convergence map is defined by

$$\kappa(\boldsymbol{\theta}) = \int \frac{\mathrm{d}^2\ell}{(2\pi)^2} \mathrm{e}^{i\boldsymbol{\ell}\cdot\boldsymbol{\theta}} \tilde{\kappa}(\boldsymbol{\ell}) \tag{8}$$

The power spectrum of the convergence map is defined by

$$\langle \tilde{\kappa}(\boldsymbol{\ell}_1)\, \tilde{\kappa}(\boldsymbol{\ell}_2) \rangle = (2\pi)^2 \delta_{\mathrm{D}}^{(2)}(\boldsymbol{\ell}_1 - \boldsymbol{\ell}_2)\, P_{\kappa\kappa}(\ell_1) \tag{9}$$

By using Limber approximation, the convergence power spectrum is described as follows:

$$P_{\kappa\kappa}(\ell) = \int_0^{\chi_s} \mathrm{d}\chi \frac{W_\kappa(\chi)^2}{r(\chi)^2} P_\delta\left(k = \frac{\ell}{r(\chi)}, z(\chi)\right) \tag{10}$$

where the lensing weight function is defined by

$$W_\kappa(\chi) = \frac{3}{2}\left(\frac{H_o}{c}\right)^2 \Omega_{\mathrm{m}0} \frac{r(\chi_s) - r(\chi)}{r(\chi_s)} (1 + z(\chi)) \,. \tag{11}$$

3.2 Peak Counts

We locate the local maxima in a smoothed lensing map and associate each identified peak with a massive dark matter halo along the same line of sight. In practice, one can select a lensing peak by its peak height. We define the signal-to-noise ratio of a peak by $\nu = \frac{K_{\mathrm{peak,\,obs}}}{\sigma_{\mathrm{noise},0}}$. For a given threshold ν_{thre}, one can predict the surface number density of peaks with $\nu > \nu_{\mathrm{thre}}$ as follows:

$$N_{\mathrm{peak}}(\nu_{\mathrm{thre}}) = \int\int \frac{dz}{dM} \frac{d^2V}{dzd\Omega} \frac{dn}{dM}(z, M) \tag{12}$$
$$\int_{\nu_{\mathrm{thre}}\sigma_{\mathrm{noise},0}}^{\infty} dK_{\mathrm{peak,\,obs}} \mathrm{Prob}(K_{\mathrm{peak,\,obs}}|K_{\mathrm{peak,\,h}}(z, M))$$

where $\frac{dn}{dM}$ represents the mass function of dark matter halo and the volume element is expressed as $\frac{d^2V}{dzd\Omega} = \frac{\chi^2}{H(z)}$ for a spatially flat universe. Here, $\mathrm{Prob}(K_{\mathrm{peak,\,obs}}|K_{\mathrm{peak,\,h}})$ is given by equation.

3.3 Maths

4 CONCLUSIONS

ACKNOWLEDGEMENTS

The Acknowledgements section is not numbered. Here you can thank helpful colleagues, acknowledge funding agencies, telescopes and facilities used etc. Try to keep it short.

DATA AVAILABILITY

The inclusion of a Data Availability Statement is a requirement for articles published in MNRAS. Data Availability Statements provide a standardised format for readers to understand the availability of data underlying the research results described in the article. The statement may refer to original data generated in the course of the study or to third-party data analysed in the article. The statement should describe and provide means of access, where possible, by linking to the data or providing the required accession numbers for the relevant databases or DOIs.

5 CITATION

Sato et al. (2009), Shirasaki et al. (2015)

REFERENCES

Bayer A. E., Liu J., Terasawa R., Barreira A., Zhong Y., Feng Y., 2023, Phys. Rev. D, 108, 043521
Osato K., Liu J., Haiman Z., 2021, Monthly Notices of the Royal Astronomical Society, 502, 5593
Sato M., Hamana T., Takahashi R., Takada M., Yoshida N., Matsubara T., Sugiyama N., 2009, The Astrophysical Journal, 701, 945
Shirasaki M., Hamana T., Yoshida N., 2015, MNRAS, 453, 3043

APPENDIX A: SOME EXTRA MATERIAL

If you want to present additional material which would interrupt the flow of the main paper, it can be placed in an Appendix which appears after the list of references.

This paper has been typeset from a TEX/LATEX file prepared by the author.